

University of Wollongong

## Research Online

---

Australian Institute for Innovative Materials -  
Papers

Australian Institute for Innovative Materials

---

1-1-2015

### Two-step self-assembly of hierarchically-ordered nanostructures

Qiannan Liu

*University of Wollongong*, ql953@uowmail.edu.au

Ziqi Sun

*University of Wollongong*, ziqi@uow.edu.au

Yuhai Dou

*University of Wollongong*, yd930@uowmail.edu.au

Jung Ho Kim

*University of Wollongong*, jhk@uow.edu.au

S X. Dou

*University of Wollongong*, shi@uow.edu.au

Follow this and additional works at: <https://ro.uow.edu.au/aiimpapers>



Part of the [Engineering Commons](#), and the [Physical Sciences and Mathematics Commons](#)

---

#### Recommended Citation

Liu, Qiannan; Sun, Ziqi; Dou, Yuhai; Kim, Jung Ho; and Dou, S X., "Two-step self-assembly of hierarchically-ordered nanostructures" (2015). *Australian Institute for Innovative Materials - Papers*. 1476.  
<https://ro.uow.edu.au/aiimpapers/1476>

Research Online is the open access institutional repository for the University of Wollongong. For further information contact the UOW Library: [research-pubs@uow.edu.au](mailto:research-pubs@uow.edu.au)

---

## Two-step self-assembly of hierarchically-ordered nanostructures

### Abstract

Due to their unique size- and shape-dependent physical and chemical properties, highly hierarchically-ordered nanostructures have attracted great attention with a view to application in emerging technologies, such as novel energy generation, harvesting, and storage devices. The question of how to get controllable ensembles of nanostructures, however, still remains a challenge. This concept paper first summarizes and clarifies the concept of the two-step self-assembly approach for the synthesis of hierarchically-ordered nanostructures with complex morphology. Based on the preparation processes, two-step self-assembly can be classified into two typical types, namely, two-step self-assembly with two discontinuous processes and two-step self-assembly completed in one-pot solutions with two continuous processes. Compared to the conventional one-step self-assembly, the two-step self-assembly approach allows the combination of multiple synthetic techniques and the realization of complex nanostructures with hierarchically-ordered multiscale structures. Moreover, this approach also allows the self-assembly of heterostructures or hybrid nanomaterials in a cost-effective way. It is expected that widespread application of two-step self-assembly will give us a new way to fabricate multifunctional nanostructures with deliberately designed architectures. The concept of two-step self-assembly can also be extended to syntheses including more than two chemical/physical reaction steps (multiple-step self-assembly).

### Keywords

hierarchically, ordered, assembly, self, step, two, nanostructures

### Disciplines

Engineering | Physical Sciences and Mathematics

### Publication Details

Liu, Q., Sun, Z., Dou, Y., Kim, J. & Dou, S. Xue. (2015). Two-step self-assembly of hierarchically-ordered nanostructures. *Journal of Materials Chemistry A*, 3 (22), 11688-11699.

## Two-step self-assembly of hierarchically-ordered nanostructures

Cite this: DOI: 10.1039/x0xx00000x

Qiannan Liu,<sup>a</sup> Ziqi Sun,<sup>a,\*</sup> Yuhai Dou,<sup>a</sup> Jung Ho Kim,<sup>a</sup> and Shi Xue Dou<sup>a</sup>

Received 00th January 2012,  
Accepted 00th January 2012

DOI: 10.1039/x0xx00000x

Due to their unique size- and shape-dependent physical and chemical properties, highly hierarchically-ordered nanostructures have attracted great attention with a view to application in emerging technologies, such as novel energy generation, harvesting, and storage devices. The question of how to get controllable ensembles of nanostructures, however, still remains a challenge. This concept paper first summarizes and clarifies the concept of the two-step self-assembly approach for the synthesis of hierarchically-ordered nanostructures with complex morphology. Based on the preparation processes, two-step self-assembly can be classified into two typical types, namely, two-step self-assembly with two discontinuous processes and two-step self-assembly completed in one-pot solutions with two continuous processes. Compared to the conventional one-step assembly, the two-step assembly approach allows the combination of multiple synthetic techniques and the realization of complex nanostructures with hierarchically-ordered multiscale structures. Moreover, this approach also allows the self-assembly of heterostructures or hybrid nanomaterials in a cost-effective way. It is expected that widespread application of two-step self-assembly will give us a new way to fabricate multifunctional nanostructures with deliberately designed architectures. The concept of two-step self-assembly can also be extended to syntheses including more than two chemical/physical reaction steps (multiple-step self-assembly).

### 1. Introduction

Nanomaterials are emerging as key materials due to their novel size- and shape-dependent physical and chemical properties, which differ greatly from those of their bulk counterparts.<sup>1-6</sup> Even though there have been significant achievements in synthesizing independent zero-, one-, two-, and three-dimensional (0D, 1D, 2D, and 3D) nanostructures in the last decade, the well-controlled synthesis of complex nanostructures having both well-defined hierarchical shapes and appropriately designed constituents on multiple scales still remains a challenge.<sup>7-8</sup> Most of the characteristics of nanomaterials can be utilized and enhanced effectively when the nanomaterials are arranged in an appropriate order into 3D complex nanostructures.<sup>9-12</sup> Compared to the bulk materials with similar overall size or the constituent nanostructures, the 3D nanomaterials usually have features that combine the merits of both types of material, such as the quantum confinement effect contributed by the constituent nanostructures and the light scattering effect contributed by the larger overall size.<sup>9-12</sup>

There have been considerable advances in the techniques for achieving one- to three-dimensional arrangements on the nanoscale, on the basis of the favored “bottom-up” method in nanotechnology.<sup>13-16</sup> Unlike the “top-down” fabrication of traditional lithography, in the “bottom-up” approach, the

nanoscopic building blocks aggregate molecule by molecule (and in some cases, even atom by atom) to achieve the desired macroscopic structures and functionalities through rather weak and often specific interaction forces.<sup>17-21</sup>

The strategy of self-assembly is one of the few practical techniques which are available to obtain controllable ensembles of nanostructures based on the “bottom-up” approach. There are many excellent reviews on the self-assembly synthesis of different nanostructures.<sup>13-18, 22-29</sup> The self-assembly process, defined as the spontaneous arrangement of nanoparticles or other discontinuous components into structurally organized aggregates or networks, has been observed in a variety of examples, ranging from the formation of crystals and micelles to the formation of complex organic and organometallic molecules, through ionic bonds, hydrogen bonds, water-mediated hydrogen bonds, and hydrophobic or van der Waals interactions.<sup>17, 30-37</sup> Molecular self-assembly offers numerous attractive advantages, such as the possibility of three-dimensional assembly, the attainment of atomic feature size, and the likelihood of inexpensive mass fabrication.<sup>21, 38</sup> This approach, however, requires a high degree of control to guide the aggregation or organization of the constituent units during the solution preparation and synthesis processes.<sup>39</sup>

In the self-assembly system, surfactants have a direct effect on the growth environments of the “target” materials and help

to achieve the controllable fabrication of their nanostructures.<sup>40–42</sup> Surfactants are generally amphiphilic organic compounds containing both hydrophilic and hydrophobic groups.<sup>43</sup> Normally, surfactants are classified according to the polar head groups, which provide them with their hydrophilia, as shown in Table 1. In a bulk aqueous solution, surfactants can help reduce the surface tension of water by adsorbing at the liquid-air interface and forming specific aggregates. The major driving forces for the surfactants to form well defined aggregates are the hydrophobic attractions at the hydrocarbon-water interfaces and the hydrophilic ionic or steric repulsion between the head groups.<sup>44</sup> Surfactants have been widely used as soft templates and morphology controlling agents to fabricate desired nanostructures.<sup>45–47</sup> Surfactant-directed synthesis can help to prepare monodisperse samples with narrow size distributions, low tendency towards agglomeration, excellent control over crystal size, good control over crystal shape, and good redispersibility.<sup>48, 49</sup> In this concept paper, the molecular self-assembly involved in the two-step self-assembly is mainly surfactant-assisted self-assembly.

Table 1 Classification of surfactants.

| Classification        | activity source   | most used                                      |
|-----------------------|---|--|
| cationic surfactant   | hydrophilic cations with nitrogen, sulphur, phosphorus              | amines, quaternary ammonium                    |
| anionic surfactant    | hydrophilic anions  | carboxylates, sulfonates, sulfates, phosphates |
| non-ionic surfactant  | multiple oxygen-containing groups, such as hydroxyl and ether bonds | polyoxyethylene, polyol                        |
| amphoteric surfactant | cations or anions   | betaines, phospholipids                        |

The design of components and their self-organization into desired structures and functions is the key to applications involving self-assembly. Molecular self-assembly has helped in the synthesis of numerous shape-defined nanostructures with 0D, 1D, 2D, and 3D dimensions. Different critical packing parameters favour the formation of different blocks, such as curved interfaces (spherical micelles and rod-like micelles), flat interfaces (flexible bilayers and planar bilayers) and inverse micelles.<sup>44</sup> Figure 1A shows the various morphologies that can be formed directly from block copolymers,<sup>50</sup> including the commercial Pluronic P123, etc. Unfortunately, synthesis via the traditional one-step self-assembly approach of hierarchically-ordered nanomaterials with controlled morphology on multiple scales is a tremendous challenge. The two-step self-assembly process is a feasible approach for refined design of hierarchically-ordered nanostructures with complex morphologies, and has been proven to be an effective way to design multiscale nanostructures, since the morphology and composition obtained from the first step can be further tuned and adjusted by a following second process. Herein, we present a detailed account of the two-step self-assembly process, with a particular focus on the surfactant-assisted two-step self-assembly synthesis of nanostructures. Based on the surfactant-water-oil phase diagram (Figure 1B),<sup>51</sup> through tuning the surfactant/water/oil ratio to the appropriate area, different hierarchical micelles constructed from (inverse) hexagonal, (inverse) cubic, and lamellar building blocks can be fabricated intentionally.

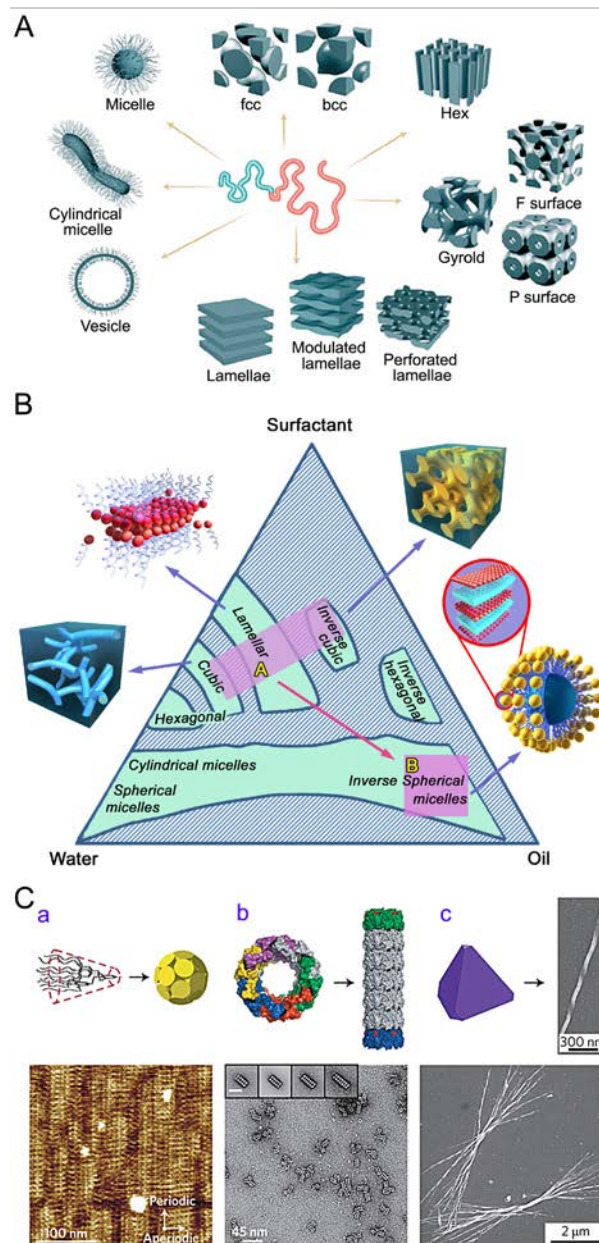


**Figure 1.** Self-assembly synthesis of hierarchically-ordered nanostructures. (A) Schematic phase diagram of the various morphologies formed by block copolymers. Reproduced with permission from Ref. 50. Copyright 2012 Royal Society of Chemistry. (B) Schematic phase diagram of surfactant–water–oil system showing the concept of two-step self-assembly in nanostructure design by first forming the desired constituent units in composition “A” and then assembling the constituent units into the final spherical morphology by adjusting the composition to “B”. Adapted with permission from Ref. 51. Copyright 2013 Tsinghua University Press and Springer-Verlag Berlin Heidelberg. (C) Hierarchical self-assembly of molecules, proteins, and nanoparticles into complex nanostructures: (a) cone-shaped monodendria self-assemble into spheres (top), which then form dendritic liquid quasicrystals (bottom); (b) hexameric ring structures self-assembled from protein building blocks (top left: with different colors indicating different protein subunits) form short nanotubes (top right and bottom); (c) truncated semiconducting CdTe tetrahedra (top left) self-assemble into twisted nanoribbons (top right), which, in turn, assemble into polydisperse bundles (bottom). Reproduced with permission from Ref. 13. Copyright 2014 Nature Publishing Group.

A specific two-step molecular self-assembly concept was thus proposed by Sun *et al.*<sup>51,52</sup> In this two-step process, the oligomers or the constituent nanostructured blocks are first synthesized from structure-defined surfactant micelles (the composition in area A), and then the obtained constituent blocks are further assembled into the final structures with the help of an oil-like surfactant that acts as a co-surfactant to tailor the solution composition into area B.<sup>51,52</sup> Complex biological nanostructures and supramolecular compounds, as well as inorganic nanoparticles, as in the examples presented in Figure 1(C),<sup>13</sup> have been fabricated by hierarchical two-step self-assembly. Similarly, more complex structures, such as yolk-shell structures with multiple layers or multiple core-shell structures, can be synthesised from several self-assembly processes or together with other methods.<sup>53-55</sup>

## 2. Overview of two-step self-assembly synthesis

Two-step self-assembly is used to fabricate many desired structures, including mesostructures, composite films, colloidal particles, hierarchical nanostructures, etc., from either two independent processes or from a one-pot solution with continuous processes. The concept of “two-step assembly” was firstly proposed in 1985 by Yurchenco *et al.* for the self-assembly of laminin into large polymers, in which the overall self-assembly of laminin was divided into two-steps: an initial divalent-cation-independent, temperature-dependent step followed by a subsequent divalent-cation-dependent step induced by the addition of ethylene diamine tetraacetic acid (EDTA).<sup>56</sup> Based on the preparation processes, two-step self-assembly can be classified into two typical types, namely, two-step self-assembly with two discontinuous processes, and two-step self-assembly completed in one-pot solutions with two continuous processes.

Compared to the conventional one-step assembly, application of the two-step assembly approach allows the combination of multiple synthetic techniques and the realization of hierarchically-ordered nanostructures with complex multiscale structures. Moreover, this approach also allows the self-assembly of heterostructures or hybrid nanomaterials in a cost-effective way. It is expected that the widespread promotion of two-step self-assembly will give us a new way to fabricate multifunctional nanostructures that integrate deliberately designed functionalities on each constituent scale. The concept of two-step self-assembly can also be extended to syntheses including more than two chemical/physical reaction steps (multiple-step self-assembly).

### 2.1. Two-step self-assembly with two discontinuous processes

The term “two-step self-assembly with two discontinuous processes” indicates that at least one step comes from the self-assembly approach, while the other step may be completed via self-assembly or other methods, such as lithography, to modify the products obtained in the first step, or vice versa. The critical feature of two-step self-assembly with two discontinuous processes is that the product of the first process is visible or detectable and can be modified by the following second step. This method has been widely used for the fabrication of complex nanostructures and other ordered structures.<sup>56-68</sup> Based on the synthetic methods employed, two-step self-assembly with two discontinuous processes can be classified into two types: discontinuous two-step self-assembly with two self-

assembly processes, or self-assembly with one step, while the other step is based on other techniques.

#### 2.1.1. Discontinuous two-step self-assembly with two self-assembly processes

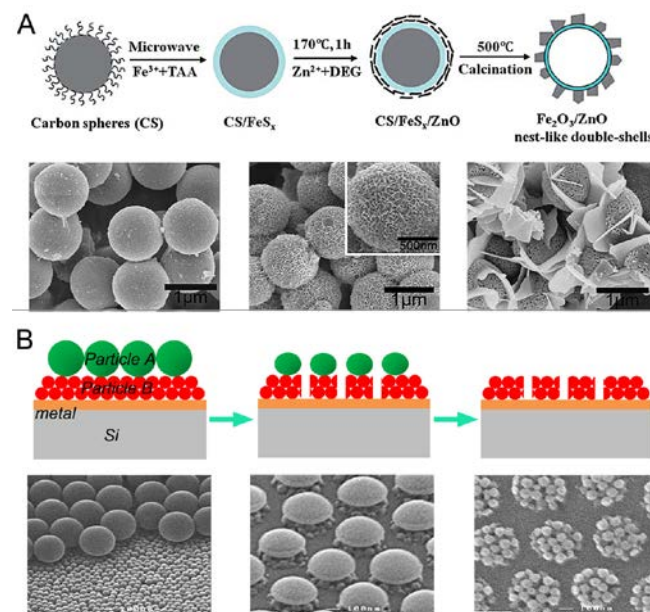


**Figure 2.** Two-step self-assembly with two discontinuous processes. (A) Schematic illustration of the formation of  $\gamma$ - $\text{Fe}_2\text{O}_3/\text{ZnO}$  double-shelled hollow nanostructures via two independent self-assembly steps, and the corresponding microstructure evolution. Adapted with permission from Ref. 59. Copyright 2012 Royal Society of Chemistry. (B) Schematic illustration of the preparation of hierarchical patterned arrays of nanoparticles by using a combination of colloidal lithography and self-assembly, and the corresponding microstructure evolution. Adapted with permission from Ref. 70. Copyright 2008 American Chemical Society.

The first example of two-step self-assembly with two discontinuous processes is where the synthesis is accomplished by using two self-assembly processes.<sup>57-59</sup> This method has been used to prepare 3D porous wormhole-structured MSU-X mesoporous silica.<sup>57</sup> In this case, the reaction was composed of a first assembly between non-ionic poly(ethylene oxide) (PEO) micelles and silica oligomers, which was then followed by a condensation induced by sodium fluoride. In the assembly process, a low-density framework of silica grows out of the micellar hydrophilic outer shell composed of PEO chains and builds a third shell around the initial spherical micelle.

Xu *et al.* reported the synthesis of well-ordered mesoporous structured resorcinol–formaldehyde polymer and carbon.<sup>58</sup> In the synthesis, formaldehyde and resorcinol are pre-polymerized and assembled in the first step with the addition of a basic catalyst to produce resorcinol–formaldehyde resol. Then, after mixing with Pluronic F127 surfactant solution, the resorcinol–formaldehyde resol achieves rapid self-assembly and condensation with the help of an acid catalyst in the second step. Compared to the one-step self-assembly method, it was reported that the two-step self-assembly possesses the advantages of low catalyst usage and room temperature synthesis.



Magnetic nest-like  $\gamma$ -Fe<sub>2</sub>O<sub>3</sub>/ZnO double-shelled hollow nanostructures have been successfully synthesized via a multi-step process, in which two self-assembly steps are included.<sup>59</sup> As shown in Figure 2(A), in the first step, a layer of FeS<sub>x</sub> is coated on the surface of colloidal carbon spheres (CS) with the help of thioacetamide (TAA) by a microwave irradiation technique. Then, the as-prepared C/FeS<sub>x</sub> nanocomposites and zinc acetate dehydrate are mixed in diethylene glycol (DEG) to obtain the sandwiched nanostructures of C/FeS<sub>x</sub>/ZnO. Finally, the composite is calcined in air to obtain the  $\gamma$ -Fe<sub>2</sub>O<sub>3</sub>/ZnO nest-like double-shelled hollow nanostructures. It has to be pointed out that the two-step assembly included in the synthesis results in this highly ordered hybrid nanocatalyst, which presents very high visible-light photocatalytic activity towards the degradation of different organic dyes.

Moreover, the self-assembly of bimetallic systems with cores or seeds is also within the scope of a discontinuous two-step approach with two self-assembly processes, in which the cores or seeds are first synthesized, and then are transferred into the second solution to form the shell or outer layer structures, such as in the synthesis of Pd on Au reported by Lim *et al.*<sup>60-62</sup>

### 2.1.2. Discontinuous two-step self-assembly with one self-assembly step together with other techniques

The second type of two-step self-assembly with two discontinuous processes is the synthesis of nanostructures by combining self-assembly with other techniques, such as lithography, hydrolysis, carbonization, etc., which has been studied much more widely than the first type.<sup>63-68</sup>

The first example is the type of synthesis with one template-assisted self-assembly followed by the removal of templates. Polycrystalline CdS nanotubes were synthesized by first depositing CdS onto anodic alumina membrane (AAM) templates and then removing the templates.<sup>63</sup> In detail, pure metal Cd nanowires were firstly electrodeposited inside the nanochannels of the AAM templates, and then the outer walls of the Cd nanowires were sulphurised under sulphur atmosphere to form a CdS layer. Secondly, the CdS nanotubes were obtained by removing the excess Cd and the AAM templates. Via a similar method, self-assembly of high-density Al<sub>2</sub>O<sub>3</sub> nanodots on SiO<sub>2</sub> was reported by depositing Al film on a SiO<sub>2</sub> layer formed on *p*-type Si (100) wafers, followed by an annealing in ambient N<sub>2</sub> to form Al nanodots, and then an oxidization of the Al nanodots to Al<sub>2</sub>O<sub>3</sub> nanodots, resulting in improved retention properties compared to those with Al<sub>2</sub>O<sub>3</sub> continuous films.<sup>64</sup> Some noble metal mesoporous structures have also been synthesized by this two-step approach using a mesoporous silica template.<sup>65</sup> Basically, most hard-template assisted self-assembly of nanostructures can be included in this two-step approach.

Ordered mesoporous Fe<sub>2</sub>O<sub>3</sub>@C encapsulates with novel nano-architectures have been rationally designed and fabricated by using a pre-hydrolysis post-synthetic route.<sup>66</sup> In this example, bimodal mesoporous carbon is used as template to load hydrated iron nitrate precursor. The obtained mesoporous Fe<sub>2</sub>O<sub>3</sub>@C encapsulates from in-situ hydrolysis and pyrolysis exhibit superior performance for arsenic capture to those prepared by direct pyrolysis. Long-range ordered organosilica and carbon-silica hybrids with uniform morphology have also been produced by hydrolysis and self-assembly of biphenyl bridged organosilane in the presence of a Pluronic P123 surfactant, followed by thermal polycondensation and carbonization.<sup>67</sup> The presence of P123 here is decisive in

obtaining uniform crystals, as a result of its assistance with the dispersion of the hydrophobic precursors in water.

Recently, uniform yolk-shell structured carbon spheres with a hierarchical porous nano-architecture have been successfully synthesized through a new gradient sol-gel process with surfactant-directing co-assembly by using the cationic surfactant cetyltrimethylammonium bromide (CTAB) as the template, resorcinol-formaldehyde (RF) as the carbon source and tetraethoxysilane (TEOS) as an assistant pore-forming agent, followed by carbonization and silica removal.<sup>68</sup>

Besides monodisperse nanostructures, many other structures, such as colloidal particles and composite films, have been prepared through self-assembly together with other approaches.<sup>69-73</sup> A combined technique of self-assembly and pattern transfer was used to realize pattern formation of gold nanoparticles.<sup>69</sup> In this study, dot and line patterns of nanoparticles were created on a template substrate (SiO<sub>2</sub>/Si) by utilizing template-assisted self-assembly. The obtained patterns of nanoparticles were then transferred to a flexible polydimethylsiloxane (PDMS) substrate (the first transfer) and subsequently transferred onto a gold thin film deposited on a silicon substrate (the second transfer).

Hierarchical nanoparticle arrays of silica nanospheres, polystyrene (PS) microspheres, and film patterns were obtained through a combination of colloidal lithography and self-assembly.<sup>70</sup> In this approach, as shown in Figure 2(B), a uniform nanoparticle film (~15-50 nm in diameter) is firstly deposited on a substrate. Then, larger microparticles (several hundreds to thousands of nanometers in diameter) with different compositions are assembled into highly ordered patterns on the surface of the nanoparticle film. After the initial nanoparticle film is partly removed and the remaining upper layer of large particles is selectively removed, hierarchical nanoparticle patterns are finally produced on the flat surface.

Hattori *et al.* prepared a polymer-particle composite film composed of commercially available polyelectrolytes, including poly(diallyldimethylammonium chloride) (PDMA) and colloidal titania (TiO<sub>2</sub>) or silica (SiO<sub>2</sub>) particles.<sup>71</sup> This process consists of coating a polyelectrolyte onto a substrate and then immersing the coated substrate in a particle suspension. Similarly, Mino *et al.* assembled silica colloidal particles into a network pattern by a combination of immersion and self-assembly.<sup>72</sup> In this approach, grid-patterned stripes of silica colloidal particles are initially fabricated on a substrate through dipping it into a suspension. Then, the substrate with the stripes is rotated by 90° and again immersed in the suspension to produce stripes perpendicular to the first ones.

Self-assembly growth of ZnO-based radial and axial junctions was reported by chemical vapour deposition (CVD) and a subsequent aqueous self-assembly process.<sup>73</sup> Pure or doped ZnO microrods were initially fabricated by the CVD method, which was subsequently followed by an aqueous solution method for further growth of the ZnO-based junctions.

### 2.2. Two-step self-assembly with two continuous processes

In the second type of two-step self-assembly, the 'two-step' process is initiated and completed in a one-pot solution via two continuous processes. During the synthesis, the self-assembly processes, particularly the second step, take place spontaneously and are induced by different driving forces, such as interfacial reactions, oriented aggregation, Ostwald ripening, and hydrophobic interactions of the building blocks.

### 2.2.1. Interfacial interaction-driven two-step self-assembly

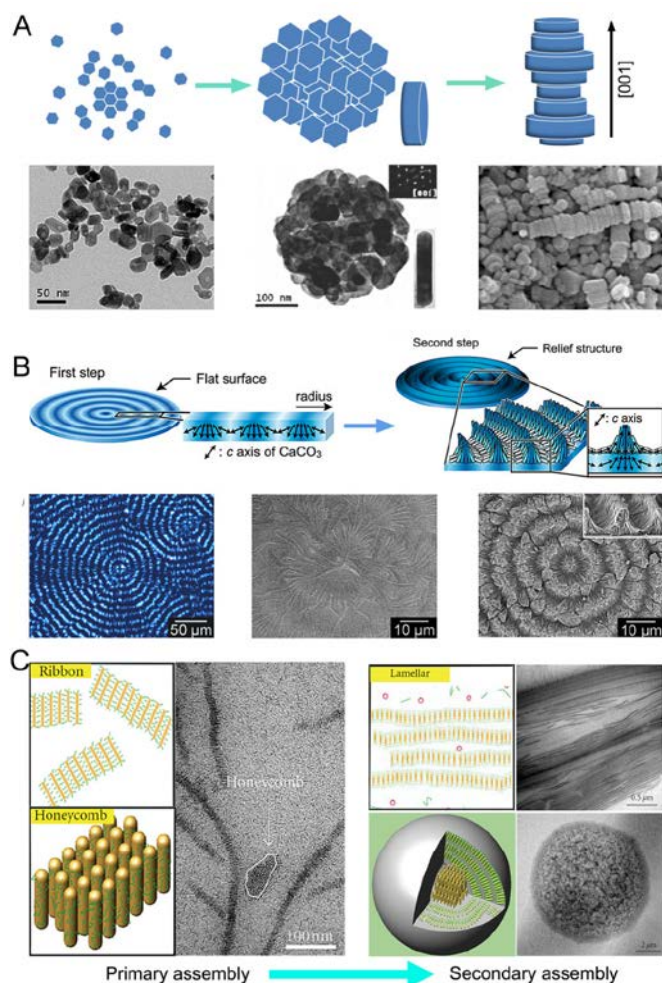


**Figure 3.** Two-step self-assembly of nanostructures via two continuous processes. (A) Schematic illustration of the assembly of LaF<sub>3</sub> nanodisks with cavities into cylinders composed of plates, driven by oriented aggregation and Ostwald ripening, and the corresponding microstructure evaluation. Adapted with permission from Ref. 77. Copyright 2005 American Chemical Society. (B) Schematic illustration of the formation of 3D CaCO<sub>3</sub> relief structures driven by crystal growth forces, and the corresponding polarized optical image and SEM images of CaCO<sub>3</sub> crystals grown on polyvinyl alcohol (PVA) matrices. Adapted with permission from Ref. 85. Copyright 2009 American Chemical Society. (C) Schematic illustration of the formation of hierarchical spherulites and lamellar TiO<sub>2</sub> nanostructures, driven by anisotropic attractive forces and gravity, respectively, and the corresponding microstructure evaluation. Adapted with permission from Ref. 88. Copyright 2012 Hindawi Publishing Corporation.

The two continuous self-assembly processes can be completed and driven by interfacial interactions among constituent units. Lu et al. proposed a two-step assembly strategy to construct ZnO 3D superstructures, in which a robust and stable gas/liquid interface formed from H<sub>2</sub>O<sub>2</sub> and dimethylsulphoxide (DMSO) organic solvent was employed to confine the crystallization and drive the assembly process.<sup>74</sup> In this case, the ZnO nanorod building blocks with diameters ranging from 100 to 200 nm

were first assembled to form microspheres, and then these microsphere units were further connected in a linked side-by-side manner in a secondary assembly process to generate the ultra-large 3D superstructure. In another case, at an air/water interface, ordered 2D arrays of β-HgS nanocrystals were aggregated through the interfacial reaction between H<sub>2</sub>S in the gaseous phase and Hg<sup>2+</sup> in the subphase in the presence of liquid-expanded monolayers of arachidic acid (AA).<sup>75</sup> The thus-formed HgS nanocrystals spontaneously assembled into round aggregates due to the interactions with AA molecules, and the aggregates further assembled into 2D arrays.

Self-assembly of different hierarchical organic nanostructures on each side of a supramolecular film, by using hydrogen-bonding interactions between tetrapyrrolylporphyrin (TPyP) and benzene-1,3,5-tricarboxylic acid (BTC) at the H<sub>2</sub>O/CHCl<sub>3</sub> interface, were successfully achieved.<sup>76</sup> The surface of the film that faces water is composed of nanoprism arrays, whereas the surface facing CHCl<sub>3</sub> consists of three-dimensional sunflower-like hierarchical micro- and nanostructures. Each side of the film also exhibits distinct soakage properties.

### 2.2.2 Oriented aggregation and/or Ostwald-ripening-driven two-step self-assembly

Oriented aggregation, which often works together with the Ostwald ripening process, of the building blocks can also help to realize the continuous two-step self-assembly of desired structures. Figure 3(A) shows the oriented aggregation-based two-step self-assembly of hexagonal LaF<sub>3</sub> nanodisks into cylinders composed of stacked plates in acidic solution.<sup>77</sup> Firstly, the nanodisks sequentially self-assembled into monocrystalline plates by coalescence, mainly resulting from the oriented aggregation of {100} planes, followed by Ostwald ripening to smooth their surfaces. Secondly, the plates with smooth surfaces were stacked face-to-face along the [001] direction to construct the 3D cylinders.

Liu et al. reported the synthesis of 3D CuO hierarchical microspheres with nanosheet subunits, which involves two stages: tiny nanoplates attached side by side first assemble themselves into 2D nanosheets via an orientation attachment growth mode, and the as-formed sheets assemble in an orderly manner and align themselves radially from the center through layer-by-layer growth to form well-defined microspheres with a multilayered structure.<sup>78</sup>

Bi<sub>2</sub>WO<sub>6</sub> with multilayered disc-like and 3D hierarchical nest-like architectures self-assembled from 2D nanosheets were successfully synthesized. When the amount of added EDTA is 0.20 g, the thus-formed nanoplates are interconnected in an edge-to-edge manner along the [001] direction, and then the microdiscs stack to form flat multilayered disks in a layer-by-layer growth style, and undergo the Ostwald ripening process to minimize the interfacial energy. When the amount of EDTA is increased to 0.40 g, the nanoplates assemble in an imperfect oriented-attachment manner and cause some misorientations in the interfaces between these nanoplates, resulting in the assembly of tilted nanoplate-based nest-like structures.

Quite recently, ZnSe nanorod loops with uniform pairs of parallel nanorods bridged at their ends were obtained from individual <sup>80</sup>ZnSe nanoparticles via a two-step self-assembly technique. The nanorods were firstly fabricated from the self-assembly of individual ZnSe nanoparticles by oriented attachment. Driven by van der Waals forces, and perhaps other attractive forces such as dipolar and charge-pairing interactions,

the nanorods then formed loosely bound pairs. When the temperature was increased, short caps that bridged the two ends of the pair were formed, due to activation of the ends of the paired rods.

Through interacting with zinc species, polyethylene glycol (PEG) molecules were reported to aggregate into globules and englobe the zinc species to form ZnO nanostructures.<sup>81</sup> The single crystalline ZnO nanoprisms aggregate into urchin-type globules on the microscale with PEG 2000 used as directing reagent, while spherical aggregates of single crystalline ZnO nanocones are obtained under the direction of PEG 200. The globules with flagella are templates for the assembly of the ZnO nanotubes or ZnO nanocones, by the mechanism of oriented-attachment and Ostwald ripening. 3D Fe<sub>3</sub>O<sub>4</sub>/α-FeOOH porous hollow microspheres with nanosheet constituents were also synthesized through two-step self-assembly induced by the Ostwald ripening process.<sup>82</sup> The Fe<sub>3</sub>O<sub>4</sub>/α-FeOOH microspheres were composed of nanosheets resulting from the self-assembly of Fe<sub>3</sub>O<sub>4</sub> nanoparticles and Fe<sub>3</sub>O<sub>4</sub>/α-FeOOH nanoneedles, and the hollow structure was formed by the complete consumption of the core in the center of each microsphere via the Ostwald ripening process.

### 2.2.3 Hydrophobic interaction-driven two-step self-assembly

Induced by hydrophobic interactions of preformed tetrameric elementary micelles, hierarchically dumbbell-shaped amphibifullerenes were reported to assemble in aqueous solution and form spherical or rod-like aggregates with recurring structural motifs.<sup>83</sup> In this example, small particles 3–4 nm in diameter were first formed from hydrophilic substituted bifullerene derivatives and continued to aggregate towards higher architectures in the case of the amphiphilic substituted bifullerenes. The second aggregation step is directed by the exposure of the hydrophobic surfaces due to the reduced number of hydrophilic substituents.

In another example, through precise tuning of the ratio of silk to elastin, different structures of silk-elastin-like polymers have been synthesized.<sup>84</sup> The synthesis consists of spontaneous formation of micellar-like particles driven by hydrogen bonding between the silk blocks, and thermal responsive self-assembly of these particles into reversible coacervates or irreversible gel states driven by the hydrophobic interaction between elastin blocks above a specific transition temperature.

### 2.2.4 Two-step self-assembly induced by other driving forces

Besides the driving forces of two-step self-assembly presented above, the second self-assembly process can be induced by other factors, such as selective crystal growth, attractive interactions, reduction potential difference, gravity, anion coordination protocols, etc.<sup>85-91</sup>

With the tendency to grow up, a three-dimensional relief structure of CaCO<sub>3</sub> was obtained by two-step crystal growth on a poly(vinyl alcohol) (PVA) matrix in the presence of poly(acrylic acid) (PAA).<sup>85</sup> As Figure 3(B) shows, the first step is self-organization of thin-film crystals with flat surfaces and periodic crystallographic orientations resulting from diffusion-controlled crystal growth. Then, with increasing reaction time, relief structures consisting of needlelike crystals are selectively self-assembled on the thin-film crystals obtained in the first

step, until the final formation of relief structures of CaCO<sub>3</sub> take place on the flat substrate.

Formation of bimetallic nanocompounds has been achieved through two-step self-assembly driven by the reduction potential difference between them. An Au metal core coated with a nanodendritic Pt shell (Au@Pt) was reported by Yamauchi et al.<sup>62,86</sup> Because of the different reduction potential of Au and Pt,<sup>87</sup> the Au cores are formed within a short time and the Pt deposition is then spontaneously carried out from the surfaces of the Au cores. The surfactant Pluronic F127 chains in this case could form cavities and facilitate the formation of the Pt dendrites during the Pt deposition. By intelligently employing the reduction potential difference, series of bimetallic and trimetallic systems have been synthesized quite recently, which presented superior electrochemical or catalytic performance compared to the single metallic nanostructures.

Driven by anisotropic attractive forces and gravity, respectively, two-step self-assembly of anatase TiO<sub>2</sub> nanorods was accomplished, and the nanorods were made to form different lyotropic liquid crystals in solution, including nematic, spherulitic, and lamellar phases.<sup>88</sup> Two structures were formed in honeycomb and ribbon morphology, respectively, in the initial self-assembly driven by anisotropic attractive forces. Secondary assembly occurred when the products were exposed to lower temperature, where different structures formed, as the relative amounts of honeycomb and ribbon structures changed with increasing TiO<sub>2</sub> concentration from 0.188 M to 0.262 M, as shown in Figure 3(C).

Driven by attractive interactions and solvent effects, a near-infrared cyanine dye, IR-806, was formed through assembly inside a thin veneer of dye molecules with water in a chromonic liquid crystal.<sup>89</sup> The IR-806 dye exhibits an isodesmic assembly at concentrations up to 0.1 wt %, followed by the formation of large assemblies beginning at around 0.2 wt % via a second non-isodesmic process, and is then ordered into the final liquid crystal phase.

There are some two-step self-assembly processes which are driven by atomic coordination.<sup>90-91</sup> Shape-persistent terpyridine (2, 2': 6', 2''-terpyridine ligand, TTT), with coordination to Fe<sup>2+</sup> that guides its three-dimensional self-assembly, was fabricated by the formation of nanoscale oligomeric structures (TTT•Fe) with particles around 20 nm in diameter, and there was a following self-assembly into “polymer” chains up to 5 mm long, which are stable for weeks without further precipitation.<sup>90</sup> Some core-shell bimetallic nanoparticles, such as Au@Pd, Pd@Au, Pt@Pd, Pd@Pt, etc., were also synthesized via anion coordination.

## 3. Examples of deliberate synthesis of hierarchically-ordered nanostructures via two-step self-assembly

As mentioned above, two-step self-assembly provides a versatile approach to complex nanostructure design in a controllable way. Recently, Sun et al. developed an innovative two-step self-assembly process for complex nanostructures from one-pot solutions, based on the theory shown in Figure 1B, and made a systematic study of it with experimental and theoretical verification.<sup>51, 52</sup> In the particular synthesis from two continuous self-assembly processes, specially shaped constituent oligomers or nanostructured subunits are firstly formed from structure-defined surfactant, and then the obtained architectural units are further assembled into the final morphologies in the presence of a second co-surfactant. Well-defined hierarchically-order nanostructures have been



successfully prepared using this method. Three specific examples based on this concept are presented in this part.

### 3.1. Hierarchically ordered photosensitive ZnO hollow microspheres

Based on this innovative concept, ZnO hollow microspheres with well-designed constituent units, in the shapes of 1D nanowire networks, 2D nanosheet stacks, and 3D mesoporous nanoball blocks, were successfully synthesized as novel photosensitive materials, as shown in Figure 4(A). Figure 4(B) shows the detailed differences in the morphologies and structures of the obtained ZnO hollow spheres.<sup>52</sup> In the two-step synthesis, a triblock copolymer of complex polyethylene oxide–polypropylene oxide–polyethylene oxide (PEO<sub>20</sub>–PPO<sub>70</sub>–PEO<sub>20</sub>, P123), absolute ethanol (EtOH), and deionized water with the desired surfactant–water–alcohol ratio are mixed to form a surfactant solution, and then zinc acetate dihydrate (ZnAc<sub>2</sub>•2H<sub>2</sub>O) and hexamethylenetetramine (HMTA) are added to the surfactant solution, followed by the addition of ethylene glycol (EG) to the mixed solution. Hollow spheres are finally obtained after solvothermal synthesis, followed by washing to remove the templates. Fig. 4B(a-d) shows the morphology of ZnO hollow microspheres with smooth surfaces produced by the normal one-step self-assembly, where all the chemicals are put in solution together to form inverse spherical micelles (area B in Fig. 1B) and then immediately subjected to solvothermal treatment without aging. Figure 4B(e-p) presents the morphologies of the ZnO hollow spheres synthesized via two-step self-assembly, in which the oligomers with 1D nanowire networks (Figure 4B(e-h)), 2D nanosheet stack constituents (Figure 4B(i-l)), and 3D mesoporous nanoball blocks (Figure 4B(m-p)) were first formed, and then the co-surfactant EG<sup>92</sup>

was added into the former solution to induce the further assembly of the nanostructured subunits into hollow microspheres, respectively. Alcohol (absolute ethanol in this case) has a similar effect to oil in a non-ionic surfactant-water-oil system.<sup>93</sup> HMTA can slowly release OH<sup>-</sup> ions and stimulate the hydrolysis of the precursors to form oligomers, and the isometric EG added later can induce the zinc oligomers to form cubic micelles or lamellar micelles, which self-assemble into hollow microspheres at the end. The photoelectrodes with nanostructured constituents presented strong visible light absorbance, due to the special micro-sized hollow spheres and hierarchical nanostructures on their surfaces, superior to the performance with one-step synthesized ZnO hollow microspheres with smooth and solid surfaces.

### 3.2. Bio-inspired ordered superhydrophobic ZnO hollow microspheres

In accordance with the proposed process of two-step self-assembly, complex hierarchically-ordered superhydrophobic ZnO microspheres with radial rhabdom-like structures, which were bio-inspired by fly eyes, were also synthesized by Sun and co-workers.<sup>94</sup> In the synthesis, as shown in the schematic illustration presented in Figure 5A, P123 surfactant is first added into absolute ethanol to form laminated micelles. Then, ZnO precursor solution is added to the former solution to direct the formation of radial rhabdom-like structures, which are further assembled into hollow spherical structures with the addition of EG, and finally, the hexagonal lens structure is nucleated and grown on the surfaces of the microspheres during the solvothermal synthesis process. The as-synthesized ZnO microspheres (Figure 5A(c, d)) show a similar structure to fly

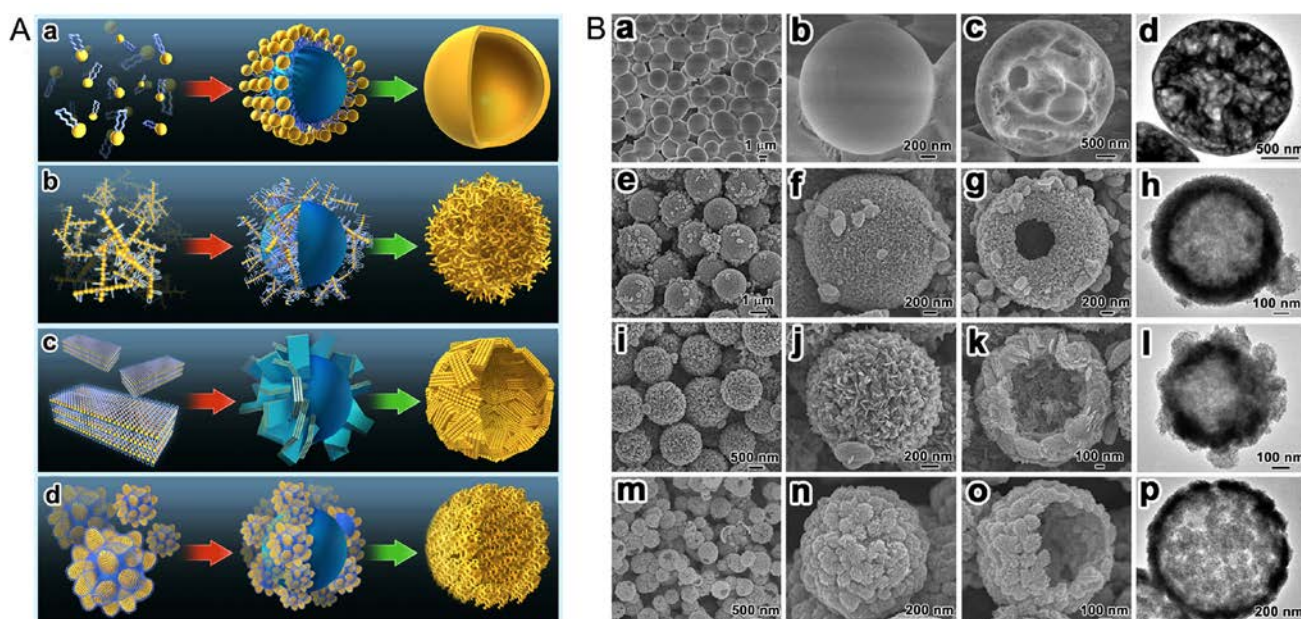


**Figure 4.** Two-step self-assembly of ZnO hollow microspheres with deliberately designed nanostructured architectures. (A) Schematic illustration of the design of ZnO hollow microspheres via a normal one-step approach (a) and via two-step self-assembly (b-d); and (B) morphologies of corresponding hollow microspheres with a smooth surface synthesized via the one-step approach (a-d), and microspheres synthesized via two-step self-assembly with designed architectures of (e-h) 1D nanowire networks, (i-l) 2D nanosheet stacks, and (m-p) 3D mesoporous nanoballs. Reproduced with permission from ref. 52. Copyright 2013 Royal Society of Chemistry.

compound eyes. The radial structures act as light-guide channels in the same way as the rhabdom does in the natural eyes, while the round hole can help achieve the incorporation of secondary optical elements inside. The bio-inspired ZnO nanostructured coating prepared by evaporation deposition of a few layers of 1H, 1H, 2H, 2H- perfluorooctyltriethoxysilane (PFOTES) molecules has excellent surface wettability and anti-fogging properties compared with bare glass, as shown in Figure 5A(d).

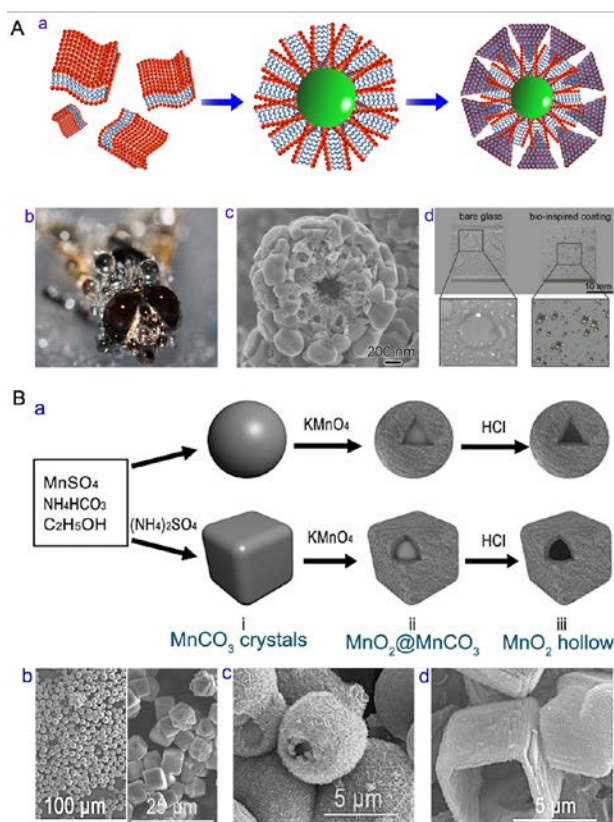


**Figure 5.** (A) Two-step self-assembly of fly-eye bio-inspired ZnO nanostructures with similar hierarchically-ordered structures to natural fly eyes, which consist of a cornea lens, a transparent crystalline cone, a rhabdom to guide light transmission, pigment cells which separate the ommatidium from its neighbours, and a central zone containing the optic nerve. (a) Schematic illustration of the two-step self-assembly of fly-eye inspired nanostructures, and (b) optical image of real fly eyes showing the feature of superhydrophobicity, (c) SEM image of the fly-eye inspired ZnO nanostructures, and (d) the superhydrophobicity of the bio-inspired nanostructured coating compared with bare glass. (B) Controlled preparation of MnO<sub>2</sub> hierarchical hollow nanostructures. (a) Schematic illustration of controlled assembly of MnO<sub>2</sub> hollow nanostructures, (b) intermediate MnCO<sub>3</sub> crystals with different morphologies, (c) MnO<sub>2</sub> shell structures with MnCO<sub>3</sub> cores, and (d) as-prepared MnO<sub>2</sub> hierarchical hollow nanostructures. Adapted with permission from ref. 94 and 95. Copyright 2014 and 2007, Wiley-VCH.

### 3.3. MnO<sub>2</sub> hierarchical hollow nanostructures

Fei et al. reported a simple method on controlled preparation of MnO<sub>2</sub> Hierarchical hollow nanostructures through self-assembly with an intermediate crystal-templating process.<sup>95</sup> As shown in Fig. 5B(a), two self-assembly steps were included in the synthesis process. First, intermediate MnCO<sub>3</sub> crystal templates with controlled morphologies in either discrete spheres or cubes were prepared by adding the (NH<sub>4</sub>)<sub>2</sub>SO<sub>4</sub> solution into the reaction solutions (Fig. 5B(b)). Then, the shells were formed on the MnCO<sub>3</sub> cores by mixing the cores with KMnO<sub>4</sub> solution (Fig. 5B(c)). The thickness of the shells can be adjusted by controlling the relative quantities of KMnO<sub>4</sub>. Finally the hollow structures can be obtained by selective removal of MnCO<sub>3</sub> crystal templates with HCl (Fig. 5B(d)). If we take the etching of the cores into account, this process can also be called as three-step synthesis.

It can be concluded that the nanostructures with hierarchical constituents can be successfully synthesized with the dimensional and functional variety accessible by this proposed concept of two-step self-assembly. The concept of two-step self-assembly can also be extended to syntheses including more than two chemical/physical reaction steps (multiple-step self-assembly).

## 4. Conclusion and outlook

Highly hierarchically-ordered nanostructures in the forms of either isolated particles or integrated films can be synthesized through the powerful two-step self-assembly approach, in which either one or both steps is based on the self-assembly process. The completion of two-step self-assembly can take place with two discontinuous processes or two continuous processes driven by different forces, or with the help of second additives. In particular, the delicate morphology of complex nanostructures with specially designed constituent units can be achieved via two-step surfactant-assisted self-assembly with continuous processes, in which the desired constituent oligomers or nanostructured subunits are firstly formed from structure-defined surfactant micelles, and then the obtained architectural units are further assembled into the final complex morphologies with the addition of a second co-surfactant. With high surface area, high chemical activity, and a quantum confinement effect, existing and possible applications for the synthesized hierarchical nanomaterials are expected to range from biomaterials to functional products such as drug delivery carriers,<sup>96</sup> catalysts, sensors, pigments, energy storage devices, and superhydrophobic materials. Also, various application of nanostructures derived from self-assembly are reviewed in several references.<sup>97-101</sup>

This two-step self-assembly can govern the self-organization of nanoparticles into hierarchically-ordered structures and ultimately integrate them into materials with the desired functions. This newly proposed concept has been proven to be effective by theoretical and experimental results for the design of hierarchically-ordered nanostructures, and will guide the design of controllable nanostructures with complex morphologies at multiple scales. It is still difficult to prepare and predict the appearance and behaviour of a certain material, however, with precise size and shape, structure, composition, and properties on the nanoscale. A detailed investigation of which organic surfactants to use and how they affect the synthetic process is essential to develop a reasonable synthesis

strategy for inorganic nanomaterials. Future attention should be paid to multicomponent systems of several different nanosized building units that are structurally and chemically synergic to fabricate unique materials or organic-inorganic hybrid nanostructures with novel properties and multifunctionality. Undoubtedly, two-step self-assembly opens up a new way to achieve rational design of novel nanomaterials with favorable architectures to meet the increasing demands on hierarchically-ordered multifunctional nanostructures with complex morphology for the emerging applications, such as novel microelectronics, next-generation sustainable energy, and advanced sensors and detectors, as well as in future healthcare.

## Acknowledgements

This work was partly supported by an Australian Research Council (ARC) Discovery Project (DP1096546) and a Discovery Early Career Researcher Award (DECRA) (DE150100280). Q. Liu is supported by funding from the China Scholarship Council, and Z. Sun acknowledges financial support from a Vice-Chancellor's Research Fellowship of the University of Wollongong, Australia and the ARC DECRA Fellowship. The authors are also grateful to Dr. Tania Silver for her critical revision of the manuscript.

## Notes and references

<sup>a</sup> Institute for Superconducting and Electronic Materials, University of Wollongong, Innovation Campus, North Wollongong, NSW 2500, Australia. E-mail: [ziqu@uow.edu.au](mailto:ziqu@uow.edu.au) OR [sun.ziqu@foxmail.com](mailto:sun.ziqu@foxmail.com)

- 1 A. Albanese, P. S. Tang, W. C. W. Chan, *Annu. Rev. Biomed. Eng.* 2012, **14**, 1.
- 2 Z. Sun, J. H. Kim, T. Liao, Y. Zhao, F. Bijarbooneh, V. Malgras, S. X. Dou, *CrystEngComm*, **2012**, 14, 5472.
- 3 B. Su, W. Guo, L. Jiang, *Small* 2015, **11**, 1072.
- 4 Y. Xia, P. Yang, Y. Sun, Y. Wu, B. Mayers, B. Gates, Y. Yin, F. Kim, H. Yan, *Adv. Mater.* 2003, **15**, 353.
- 5 Z. Sun, T. Liao, Y. Dou, S. M. Hwang, M. S. Park, L. Jiang, J. H. Kim, S. X. Dou, *Nat. Commun.* 2014, **5**, 3813.
- 6 G. M. Whitesides, *Small* 2005, **1**, 172.
- 7 J. N. Tiwari, R. N. Tiwari, K. S. Kim, *Prog. Mater. Sci.* 2012, **57**, 724.
- 8 D. Wang, T. Xie, Y. Li, *Nano Res.* 2009, **2**, 30.
- 9 Z. Q. Sun, J. H. Kim, Y. Zhao, F. Bijarbooneh, V. Malgras, Y. Lee, Y. Kang, S. X. Dou, *J. Am. Chem. Soc.* 2011, **133**, 19314.
- 10 Z. Q. Sun, J. H. Kim, Y. Zhao, D. Attard, S. X. Dou, *Chem. Commun.* 2013, **49**, 966.
- 11 P. Yang, *MRS Bull.* 2012, **37**, 806.
- 12 J. Lin, Y. Heo, A. Nattestad, Z. Q. Sun, L. Wang, J. H. Kim, S. X. Dou, *Sci. Rep.* 2014, **4**, 5769.
- 13 B. Yeom, N. A. Kotov, *Nat. Mater.* 2014, **13**, 228.
- 14 D. Long, E. Burkholder, L. Cronin, *Chem. Soc. Rev.* 2007, **36**, 105.
- 15 G. M. Whitesides, J. P. Mathias, C. T. Seto, *Science* 1991, **254**, 1312.
- 16 C. Jiang, V. V. Tsukruk, *Adv. Mater.* 2006, **18**, 829.
- 17 J. Kao, K. Thorkelsson, P. Bai, B. J. Rancatore, T. Xu, *Chem. Soc. Rev.* 2013, **42**, 2654.
- 18 Y. Liu, J. Goebl, Y. Yin, *Chem. Soc. Rev.* 2013, **42**, 2610.
- 19 X. Wang, J. Zhuang, Q. Peng, Y. Li, *Nature* 2005, **437**, 121.
- 20 J. Y. Cheng, C. A. Ross, H. I. Smith, E. L. Thomas, *Adv. Mater.* 2006, **18**, 2505.
- 21 S. Zhang, *Nat. Biotech.* 2003, **21**, 1171.
- 22 M. Law, J. Goldberger, P. Yang, *Annu. Rev. Mater. Res.* 2004, **34**, 83.
- 23 S. Ruhle, M. Shalom, A. Zaban, *ChemPhysChem* 2010, **11**, 2290.
- 24 H. Hagfeldt, G. Boschloo, L. Sun, L. Kloo, H. Pettersson, *Chem. Rev.* 2010, **110**, 6595.
- 25 G. Yu, X. Xie, L. Pan, Z. Bao, Y. Cui, *Nano Energy* 2013, **2**, 213.
- 26 Z. Chen, D. Pan, Z. Li, Z. Jiao, M. Wu, C. H. Shek, C. M. L. Wu, J. K. L. Lai, *Chem. Rev.* 2014, **114**, 7442.
- 27 G. A. Ozin, K. Hou, B. V. Lotsch, L. Cademartiri, D. P. Puzzo, F. Scotognella, A. Ghadimi, J. Thomson, *Mater. Today* 2009, **12**, 12.
- 28 J. C. Huie, *Smart Mater. Struct.* 2003, **12**, 264.
- 29 I. W. Hamley, *Nanotechnol.* 2003, **14**, R39.
- 30 G. M. Whitesides, B. Grzybowski, *Science* 2002, **295**, 2418.
- 31 Z. Quan, L. Valentin-Bromberg, W. S. Loc, J. Fang, *Chem. Asian J.* 2011, **6**, 1126.
- 32 J. Rodriguez-Hernandez, F. Chécot, Y. Gnanou, S. Lecommandoux, *Prog. Poly. Sci.* 2005, **30**, 691.
- 33 W. M. Park, J. A. Champion, *Angew. Chem., Int. Ed.* 2013, **52**, 8098.
- 34 E. Winfree, F. Liu, L. A. Wenzler, N. C. Seeman, *Nature* 1998, **394**, 539.
- 35 M. Boncheva, G. M. Whitesides, *MRS Bull.* 2005, **30**, 736.
- 36 S. Zhang, D. M. Marini, W. Hwang, S. Santoso, *Cur. Opin. Chem. Bio.* 2002, **6**, 865.
- 37 S. R. Seidel, P. J. Stang, *Acc. Chem. Res.* 2002, **35**, 972.
- 38 J. S. Lindsey, *New J. Chem.* 1991, **15**, 153.
- 39 M. Grzelczak, J. Vermant, E. M. Furst, L. M. Liz-Marzán, *ACS Nano* 2010, **4**, 3591.
- 40 W. Shi, S. Song, H. Zhang, *Chem. Soc. Rev.* 2013, **42**, 5714.
- 41 K. Holmberg, *J. Colloid Interface Sci.* 2004, **274**, 355.
- 42 H. Fan, *Chem. Commun.* 2008, **12**, 1383.
- 43 R. Dong, J. Hao, *Chem. Rev.* 2010, **110**, 4978.
- 44 J. Liu, A. Y. Kim, L. Q. Wang, B. J. Palmer, Y. L. Chen, P. Bruinsma, B. C. Bunker, G. J. Exarhos, G. L. Graff, P. C. Rieke, G. E. Fryxell, J. W. Virden, B. J. Tarasevich, L. A. Chick, *Adv. Colloid Interface Sci.* 1996, **69**, 131.
- 45 Y. Shi, Y. Wan, D. Zhao, *Chem. Soc. Rev.* 2011, **40**, 3854.
- 46 Y. Wan, D. Zhao, *Chem. Rev.* 2007, **107**, 2821.
- 47 Z. Sun, J. H. Kim, Y. Zhao, F. Bijarbooneh, V. Malgras, S. X. Dou, *J. Mater. Chem.*, **2012**, 22, 11711.
- 48 J. Park, J. Joo, S. G. Kwon, Y. Jang, T. Hyeon, *Angew. Chem., Int. Ed.* 2007, **46**, 4630.
- 49 N. Pinna, M. Niederberger, *Angew. Chem., Int. Ed.* 2008, **47**, 5292.
- 50 Y. Deng, J. Wei, Z. Sun, D. Zhao, *Chem. Soc. Rev.* 2013, **42**, 4054.
- 51 Z. Sun, T. Liao, K. Liu, L. Jiang, J. H. Kim, S. X. Dou, *Nano Res.* 2013, **6**, 726.
- 52 Z. Sun, T. Liao, J. Kim, K. Liu, L. Jiang, J. H. Kim, S. X. Dou, *J. Mater. Chem. C* 2013, **1**, 6924.
- 53 Q. Yue, Y. Zhang, C. Wang, X. Wang, Z. Sun, X. Hou, D. Zhao, Y. Deng, *J. Mater. Chem. A*, 2015, **3**, 4586.
- 54 Z. Sun, Q. Yue, Y. Liu, J. Wei, B. Li, S. Kaliaguine, Y. Deng, Z. Wu, D. Zhao, *J. Mater. Chem. A* 2014, **2**, 18322.
- 55 J. Wei, Y. Liang, X. Zhang, G. P. Simon, D. Zhao, J. Zhang, S. Jiang H. Wang, *Nanoscale* 2015, **7**, 6247.

- 56 P. D. Yurchenco, E. Tsilibary, A. Charonis, H. Furthmayr, *J. Bio. Chem.* 1985, **260**, 7636.
- 57 C. Boissière, A. Larbot, C. Bourgaux, E. Prouzet, C. A. Bunton, *Chem. Mater.* 2001, **13**, 3580.
- 58 J. Xu, A. Wang, T. Zhang, *Carbon* 2012, **50**, 1807.
- 59 Y. Liu, L. Yu, Y. Hu, C. Guo, F. Zhang, and X. Lou, *Nanoscale* 2012, **4**, 183.
- 60 B. Lim, H. Kobayashi, T. Yu, J. Wang, M. J. Kim, Z. Y. Li, M. Rycenga, Y. Xia, *J. Am. Chem. Soc.*, 2010, **132**, 2506.
- 61 C. Wang, M. Chi, D. Li, D. Strmcnik, D. van der Vliet, G. Wang, V. Komanicky, K. C. Chang, A. P. Paulikas, D. Tripkovic, J. Pearson, K. L. More, N. M. Markovic, V. R. Stamenkovic, *J. Am. Chem. Soc.*, 2011, **133**, 14396.
- 62 M. B. Gawande, R. Zboril, V. Malgras, Y. Yamauchi, *J. Mater. Chem. A* 2015, **3**, 8241.
- 63 S. M. Zhou, Y. S. Feng, L. D. Zhang, *Eur. J. Inorg. Chem.* 2003, **2003**, 1794.
- 64 J. H. Chen, W. J. Yoo, D. S. H. Chan, L.-J. Tang, *Appl. Phys. Lett.* 2005, **86**, 073114.
- 65 H. Wang, H. Y. Jeong, M. Imura, L. Wang, L. Radhakrishnan, N. Fujita, T. Castle, O. Terasaki, Y. Yamauchi, *J. Am. Chem. Soc.*, 2011, **133**, 14529.
- 66 Z. Wu, W. Li, P. A. Webley, D. Zhao, *Adv. Mater.* 2012, **24**, 485.
- 67 J. Pang, L. Yang, D. A. Loy, H. Peng, H. S. Ashbaugh, J. Mague, C. J. Brinker, Y. Lu, *Chem. Commun.* 2006, **42**, 1545.
- 68 J. Wang, S. Feng, Y. Song, W. Li, W. Gao, A. A. Elzatahry, D. Aldhayan, Y. Xia, D. Zhao, *Catal. Today* 2015, **243**, 199.
- 69 K. Sugano, T. Ozaki, T. Tsuchiya, O. Tabata, *Sensors Mater.* 2011, **23**, 263.
- 70 D. Xia, Z. Ku, D. Li, S. R. J. Brueck, *Chem. Mater.* 2008, **20**, 1847.
- 71 H. Hattori, *Thin Solid Films* 2001, **385**, 302.
- 72 Y. Mino, S. Watanabe, M. T. Miyahara, *Langmuir* 2011, **27**, 5290.
- 73 Y. Chang, Y. Lu, M. Wang, Y. Long, R. Ye, *Appl. Surf. Sci.* 2013, **264**, 687.
- 74 P. Lu, D. Xue, *Nanosci. Nanotech. Lett.* 2011, **3**, 429.
- 75 Y. G. Yang, H. G. Liu, L. J. Chen, K. C. Chen, H. P. Ding, J. Hao, *Langmuir* 2010, **26**, 14879.
- 76 N. Shi, G. Yin, M. Han, L. Jiang, Z. Xu, *Chem. Eur. J.* 2008, **14**, 6255.
- 77 Y. Cheng, Y. Wang, Y. Zheng, Y. Qin, *J. Phys. Chem. B* 2005, **109**, 11548.
- 78 X. Liu, H. Zang, J. Song, J. Tang, Y. Qian, *Asian J. Chem.* 2014, **26**, 127.
- 79 L. Xu, X. Yang, Z. Zhai, W. Hou, *CrystEngComm*, 2011, **13**, 7267.
- 80 G. Jia, A. Sitt, G. B. Hitin, I. Hadar, Y. Bekenstein, Y. Amit, I. Popov, U. Banin, *Nat. Mater.* 2014, **13**, 301.
- 81 X. Zhou, D. Zhang, Y. Zhu, Y. Shen, X. Guo, W. Ding, Y. Chen, *J. Phys. Chem. B* 2006, **110**, 25734.
- 82 Y. Jia, X. Y. Yu, T. Luo, M. Y. Zhang, J. H. Liu, X. J. Huang, *Dalton Trans.* 2013, **42**, 1921.
- 83 L. Wasserthal, B. Schade, K. Ludwig, C. Böttcher, A. Hirsch, *Chem. Eur. J.* 2014, **20**, 5961.
- 84 X. Xia, Q. Xu, G. Qin, D. L. Kaplan, *Biomacromolecules* 2011, **12**, 3844.
- 85 T. Sakamoto, A. Oichi, Y. Oaki, T. Nishimura, A. Sugawara, T. Kato, *Cryst. Growth Des.* 2009, **9**, 622.
- 86 H. Atae-Esfahani, L. Wang, Y. Yamauchi, *Chem. Commun.* 2010, **46**, 3684.
- 87 A. J. Bard, R. Parsons, J. Jordan, Standard potential in aqueous solution, *IUPAC*, 1985.
- 88 Z. Ren, C. Chen, R. Hu, K. Mai, G. Qian, Z. Wang, *J. Nanomater.* 2012, **2012**, 180989.
- 89 E. A. Mills, M. H. Regan, V. Stanic, P. J. Collings, *J. Phys. Chem. B* 2012, **116**, 13506.
- 90 J. K. Molloy, P. Ceroni, M. Venturi, T. Bauer, J. Sakamoto, G. Bergamini, *Soft Matter* 2013, **9**, 10754.
- 91 C. J. Serpell, J. Cookson, O. Ozkaya, P. D. Beer, *Nat. Chem.* 2011, **3**, 478.
- 92 R. Zana, *Adv. Colloid Interface Sci.* 1995, **57**, 1.
- 93 G. Montalvo, E. Rodenas, M. Valiente, *J. Colloid Interface Sci.* 1998, **202**, 232.
- 94 Z. Sun, T. Liao, K. Liu, L. Jiang, J. H. Kim, S. X. Dou, *Small* 2014, **10**, 3001.
- 95 J. Fei, Y. Cui, X. Yan, W. Qi, Y. Yang, K. Wang, Q. He, J. Li, *Adv. Mater.*, **2008**, **20**, 452.
- 96 Y. Li, B. P. Bastakoti, M. Lmura, J. Tang, A. Aldalbahi, N. L. Torad, Y. Yamauchi, *Chem. Eur. J.* 2015, **21**, 6357.
- 97 C. R. Lowe, *Curr. Opin. Struct. Biol.* 2000, **10**, 428.
- 98 J. H. Fendler, *Chem. Mater.* 2001, **13**, 3196.
- 99 P. Alexandridis, B. Lindman, Amphiphilic block copolymer: self-assembly and applications, *Elsevier: Amsterdam* 2006.
- 100 Y. Habibi, L. A. Lucia, O. J. Rojas, *Chem. Rev.* 2010, **110**, 3479-3500.
- 101 F. Zaera, *Chem. Soc. Rev.* 2013, **42**, 2746.